Chemical Physics Letters 489 (2010) 107–112

Contents lists available at ScienceDirect

Chemical Physics Letters

journal homepage: www.elsevier.com/locate/cplett

^{1}H NMR noise measurements in hyperpolarized liquid samples

Patrick Giraudeau [a,1], Norbert Müller [b], Alexej Jerschow [c,*], Lucio Frydman [a,*]

[a] Department of Chemical Physics, Weizmann Institute of Science, 76100 Rehovot, Israel
[b] Institute of Organic Chemistry, Johannes Kepler University, Altenbergerstraße 69, A-4040 Linz, Austria
[c] Chemistry Department, New York University, New York, NY 10003, United States

ARTICLE INFO

Article history:
Received 31 August 2009
In final form 9 February 2010
Available online 12 February 2010

ABSTRACT

Noise measurements of nuclear spin systems using a tuned circuit can reveal the signatures of two different phenomena: Thermal circuit noise absorbed by the spin system, and nuclear spin-noise leading to tiny fluctuating magnetization components. Polarization enhancement can increase the observed noise amplitudes due to an enlarged coupling with the reception circuit. In this work we explore the detection of noise in ^{1}H NMR of liquid water samples whose spin alignment is enhanced via *ex situ* dynamic nuclear polarization. A number of ancillary phenomena related to this kind of experiments are also documented.

1. Introduction

Spin-noise describes the fluctuating signals emanating from a collection of spins, and is a result of the quantum measurements of spin values. This phenomenon was predicted by Bloch in 1946 [1], but at that time could not be detected. Sleator et al. were able to measure nuclear spin-noise for the first time using a solid sample at liquid helium temperature [2,3]. Later, Ernst and McCoy [4], and independently Guéron and Leroy [5] demonstrated that spin-noise was also observable at ambient temperature with a conventional liquid-state NMR spectrometer on concentrated samples. Nuclear spin-noise was also detected optically using a technique based on Faraday rotation [6]. Recently, nuclear spin-noise was detected in the presence of magnetic field gradients along different directions and exploited for reconstrucing a two-dimensional image of the cross section of a phantom without the use of radio-frequency (rf) irradiation [7]. Spin-noise NMR could also be important in other practical applications: it has been proposed, for instance, for determining optimum tuning conditions of NMR probes [8,9]. With cryogenically cooled probes the observation of nuclear spin-noise phenomena has become relatively straightforward when dealing with large ($\sim 10^{20}$–10^{22}) numbers of spins [10,11]. The detection of spin-noise with conventional (ambient-temperature) high-resolution probes is also possible, albeit at somewhat longer accumulation times. Still, further applications of these effects are certainly limited by fundamental sensitivity issues. The quantum origins of the spin-noise phenomenon have been discussed by Hoult and Ginsberg [12].

The weakness of spin-noise NMR also raises the question of whether or not hyperpolarization techniques could be useful for amplifying the detected signals. Although the spin fluctuations or spontaneous emission probabilities should not experience any significant enhancement due to an increased spin polarization [3], the detection sensitivity could be enhanced indirectly, via an increase in the coupling to the rf-circuit (radiation damping) [13,14]. Recently, noise detection was enhanced in such fashion to enable a measurement of hyperpolarized solutions of ^{129}Xe without rf irradiation [15]. This state was generated by optical pumping [16,17]. Alternative methods that could be exploited in this kind of experiments include chemical synthesis using parahydrogen [18,19] and microwave-driven magnetization transfers from electrons to nearby nuclei by dynamic nuclear polarization (DNP) [20–23]. DNP is probably the most generally applicable among these methods, leading to signal-to-noise (SNR) enhancements of thousands or tens of thousands compared to conventional NMR [24,25]. The most natural approach to exploit the benefits of DNP within the framework of a NMR experiment would be to perform the microwave irradiation *in situ*. Although this is a method of choice for the polarization of solid state NMR signals [26], the inefficiency of the electron-nuclear spin transfer mechanisms in liquids at high field makes this procedure inappropriate to enhance signals in a high-resolution NMR setting [21,23]. An alternative way of recording DNP-enhanced liquid-state NMR data is to perform the polarization *ex situ*, at low temperatures in a glassy state, and then rapidly dissolving the sample with hot solvent vapors that concurrently transfer it to an NMR spectrometer for a conventional acquisition [24,25]. This approach has led to promising developments and applications in the field of *in vivo* NMR spectroscopy and imaging [27–30]. *Ex situ* DNP NMR was also recently combined

* Corresponding authors. Fax: +1 212 995 4475 (A. Jerschow).
E-mail addresses: alexej.jerschow@nyu.edu (A. Jerschow), lucio.frydman@weizmann.ac.il (L. Frydman).
[1] Present address: CEISAM, UMR CNRS 6230, University of Nantes, France.

0009-2614/$ - see front matter © 2010 Elsevier B.V. All rights reserved.
doi:10.1016/j.cplett.2010.02.026

with spatially-encoded ultrafast methods [31,32], leading in a single-scan to multidimensional spectra of hyperpolarized samples [33,34].

The question arises about how to distinguish spin-noise signals from noise signals originating from the absorption of circuit noise by the spins. In this work we describe a series of measurements made utilizing this *ex situ* DNP procedure, on ^{1}H NMR resonances of liquid water. Although hyperpolarization enhances the noise measurements, it does not provide the means for making this experiment more sensitive than its traditional pulsed NMR counterpart. A theoretical analysis and numerical fitting of the experimental results, however, show that the observed signals in the hyperpolarization case originate from absorbed circuit noise rather than spin-noise. Although the latter is theoretically also observable in hyperpolarized samples it would not be enhanced, and therefore would not be observable under the relatively low spin concentration conditions assayed in this work. A number of additional, interesting features emerge from studying the effects of hyperpolarization on noise measurements; these included resonance frequency shifts and line broadening phenomena arising from radiation-damping effects, which besides clarifying the noise phenomena themselves provide insight into the details of the *ex situ* DNP process.

2. Theory

A simple analysis should highlight the distinction between spin-noise (SN) and absorbed circuit noise (ACN). Starting from the basic Nyquist noise relationship one may write for the voltage spectral density according to Sleator et al. [2,3]

$$S_V(\omega) = \frac{2}{\pi} k_B [T_c R_c + T_s R_s(\omega)], \tag{1}$$

where T_c and R_c are the circuit temperature and resistance, and T_s and $R_s(\omega)$ the sample temperature and (frequency-dependent) sample resistance. The second term in this equation originates from the fluctuating magnetization components of the sample arising from SN. Sleator et al. [2,3] have further shown that for a spin-1/2 the SN term is constant regardless of spin temperature (and therefore also regardless of polarization). In any conventional measurement by a tuned circuit, however, one would measure the current spectral density

$$S_I(\omega) = \frac{2}{\pi} k_B \frac{T_c R_c + T_s R_s(\omega)}{|Z_c + Z_s(\omega)|^2} \tag{2}$$

with Z_c and Z_s denoting the circuit and sample impedances.

Before moving onto more quantifiable expressions, it is useful to investigate this equation on-resonance with negligible detuning, where $Z_c = R_c$ and $Z_s = R_s$ and one has

$$S_I(\omega) = \frac{2}{\pi} k_B \frac{T_c R_c + T_s R_s}{(R_c + R_s)^2}. \tag{3}$$

In thermal equilibrium ($T_s = T_c$), this expression predicts a 'dip' into the circuit noise. In the absence of SN, a dip would also be seen, but it would be deeper. For a hyperpolarized sample on-resonance and considering a negligible linewidth, one can write $R_s = \mu_0 \gamma L_c \eta \omega_0 K M_z$, with M_z being the thermal polarization, K the enhancement factor, η the filling factor, and L_c the circuit inductance. Since, by definition the spin-temperature T_s would be reduced by a factor K, the SN term in the numerator would remain constant. For a sizable K-factor, then, one would still observe a dip, with a negligible contribution of SN. Under these circumstances, the dip can be regarded as originating from circuit noise absorbed by the spins – absorbed circuit noise (ACN). In this Letter we refer to 'noise measurements' when we mean the measurement process and to SN and ACN when we describe the underlying mechanism. We continue with a more quantitative description of the relevant circuit equations, which will allow us to determine the conditions under which ACN and SN can be observed in polarized samples, and provide simulations fitting the experimental data.

Starting from the basic Nyquist noise relationship, McCoy and Ernst [4] and Sleator et al. [2,3] derived the expressions describing the line shapes expected from the spin-noise NMR signals. Following Eq. (10) of Ref. [4], one can modify above expressions to include a treatment of both hyperpolarized samples and cryogenically-cooled receiver circuits [9], and write the noise current spectral density as

$$S_I(\omega) = q \frac{1 + a(\Delta\omega)\lambda_r^0}{[1 + a(\Delta\omega)K\lambda_r]^2 + [d(\Delta\omega)K\lambda_r + 2Q\Delta\omega_c/\omega_c]^2}, \tag{4}$$

where $a(\Delta\omega)$ and $d(\Delta\omega)$ are the absorptive and dispersive spectral line shapes, ω_c the circuit tuning frequency, $\Delta\omega_c$ the deviation of the Larmor frequency from ω_c, and the radiation-damping rate constant of a thermally polarized sample is

$$\lambda_r = 1/T_{rd} = \frac{1}{2}\eta Q \gamma \mu_0 M_z \tag{5}$$

with η the filling factor, Q the quality factor, γ the gyromagnetic ratio, μ_0 the permeability of space, and M_z the z-magnetization of a thermally polarized sample. The modified rate constant including the temperature effect of the receiver circuit and the sample [9] is

$$\lambda_r^0 = \lambda_r \frac{T_s}{T_c} = \lambda_r \vartheta, \tag{6}$$

where T_s is the sample temperature and T_c the circuit temperature. For ambient temperature probes, $\vartheta = 1$, and for cryoprobes, $\vartheta \gg 1$.

It was recently reported that under on-resonance tuning conditions, both negative ('dips') and positive ('bumps') noise power signals can be observed on top of the thermal noise in experiments involving cryoprobes [9]. In analogy to the derivation of Eqs. (11)–(14) of Ref. [4] and Eq. (5) of Ref. [9], one can define the condition for measuring noise absorption peaks (dips) at the noise tuning optimum

$$\lambda_2 \left(\frac{\vartheta}{K} - 2\right) < K\lambda_r \tag{7}$$

with $\lambda_2 = 1/T_2^*$ (assuming Lorentzian lineshapes), where T_2^* is the transverse relaxation time including both homogeneous and inhomogeneous contributions. A bump always indicates SN (in particular, a bump is always seen for a saturated sample), while a dip will have contributions from both ACN and SN. Eq. (7) indicates that, when the enhancement is large ($K \gg 1$), noise signals will appear in the form of dips in both room temperature and cryoprobes. Lowering the circuit temperature further increases the contribution of SN, while enhancement of polarization increases the contribution of ACN. We set out to explore the latter changes by means of *ex situ* liquid-state ^{1}H DNP NMR.

3. Experimental

The samples examined in the DNP experiments were prepared by dissolving 4-Oxo-TEMPO (Aldrich) in a 1:1 H_2O:DMSO-d_6 v/v mixture (Cambridge Isotope Laboratories), so as to yield a 30 mM radical concentration. For the spin-noise experiments 200 μL of this solution were used; 50 μL aliquots of the same mixture were also used for studying the decay of the H_2O NMR signal after hyperpolarization. To perform the DNP enhancement these samples were placed inside the helium-cooled variable-temperature insert located inside a 3.35 T Hypersense® polarizer (Oxford Instruments). These glass-forming samples were then cooled to 1.4 K, and irradiated for 15 min at 94.08 GHz with a microwave power of 100 mW, after which the solid-state probe indicated that a

polarization plateau was reached. Following its hyperpolarization, the sample was suddenly dissolved in pre-heated D_2O vapors (Cambridge Isotope Laboratories), and chased with a 5 atm 99.999% He gas stream into the NMR tube located within the magnet. Additional tests revealed that the actual solvent volume to which the hyperpolarized samples were diluted in these cases equaled approximately 2.2 mL. The transfer time between dissolution and arrival in the NMR tube was determined to be 0.75 s. The temperature of the solution in the NMR tube was determined to be 312 K by measuring the frequencies of injected solutions of water and methanol. Additional spectroscopic imaging measurements revealed that a temperature gradient across the sample, if present, would not have been in excess of 2 K.

The NMR measurements themselves were carried out on an 11.7 T Varian Inova spectrometer, equipped with a 5 mm probe including triple axis gradients. For all experiments, the probe was detuned by −1.3 MHz with respect to the ^{1}H resonance frequency to reach the spin-noise tuning optimum (SNTO) [9]; this is the reception-tuning condition [8], and its value was chosen so as to obtain a purely negative dip for spin-noise experiments. The quality factor Q of the probe was determined from the tuning curve as 190. For the spin-noise experiments, the transmitter cable was disconnected from the ^{1}H amplifier while the NMR data were acquired. Spin-noise acquisitions lasted 8 s for conventionally-polarized samples and 16 s for the DNP-enhanced ones; in all cases, data were sampled over a 2 kHz spectral width (500 μs dwell times between the complex-valued data points). The resulting acquired data string was exported from the spectrometer, spliced into 2000-point arrays, and Fourier-transformed in power spectrum mode (square of absolute value). Eight consecutive power spectra were subsequently co-added to improve the overall signal-to-noise ratio (SNR). Ancillary DNP-enhanced NMR experiments were also recorded; these data acquisitions were started a few seconds prior to the sample's dissolution and ejection from the hyperpolarizer, so as to allow for a more precise determination of the initial sample injection moment. These measurements were aimed at characterizing the behavior of the ^{1}H liquid signal after concluding the hyperpolarization; toward this end a total of 1000 NMR signals were recorded on DNP-enhanced samples using 0.8 degree excitation pulses (pulse duration 1 μs), an acquisition time of 0.2 s (50 μs dwell time), and no delays between scans. All processing was performed using Matlab®.

4. Results and discussion

As a first step in this spin-noise analysis, the enhancement factor K involved in Eq. (4) was independently determined. To do so, a series of small flip-angle NMR experiments was collected, as a function of time elapsed following a DNP-enhanced sample injection. The integral of the resulting signals should yield a reliable indicator of the relative enhancement factor, and when compared to the integral at thermal equilibrium, it should yield the absolute value of this enhancement. Fig. 1 illustrates the typical time progression observed for the resulting ^{1}H NMR spectra, plotted in 4 s increments and in a normalized fashion. Two main features are apparent from this time progression. One is the large linewidth of the resulting peak; reaching up to ~1190 Hz at very short times following the injection, and decreasing to normal values of a thermally polarized sample afterwards. This effect was initially thought to be mainly a result of large ΔB_o field inhomogeneities associated with air/gas bubbles arising upon executing the sudden sample injection. On the other hand, in the strong radiation-damping regime, the linewidth is dominated by the radiation-damping time constant. Therefore, if $K\lambda_r \gg \lambda_2$ the linewidths of these spectra would be dominated on $K\lambda_r$. Hence, the resulting widths should

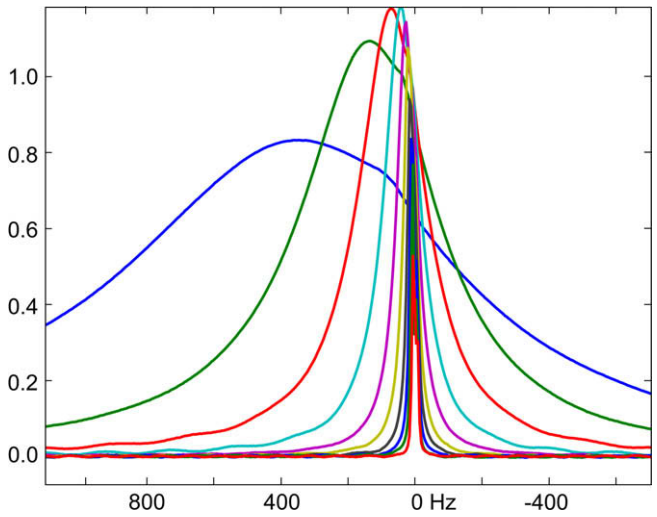

Fig. 1. Small flip angle (0.8°) spectra of hyperpolarized water signals after injection into the NMR spectrometer, at 4 s intervals. After injection, the signals narrow and the frequency shifts as discussed in the text.

also correlate with the polarization's progressive time decrease; this behavior is indeed experimentally observed. Still, it should be noted that these radiation-damping effects should result in a symmetric broadening of the resonance; some of the asymmetries evidenced at short times by the peaks shown in Fig. 1, should therefore be assigned to heterogeneities that have not yet settled after the sample is injected. A second remarkable feature evidenced by the DNP-enhanced ^{1}H resonances in Fig. 1 is the appearance of clear shifts that the resonances undergo as a function of time following the sample injection. Although shifts may be expected due to nuclear-spin-induced dipolar fields [35], such effects would be minor (up to ~14 Hz at the observed enhancement factors). At this point it is much more likely that these shifts are caused by radiation-damping induced shifts [13,36,37], which decrease over the course of time as the spin polarization decays. Independent experiments at variable microwave irradiation times show that an overall good correlation between linewidths, frequency shifts, and polarization levels is indeed observed, even if inhomogeneities partly mask these effects – especially at early times after injection.

Fig. 2 summarizes the relevant aspects of these DNP-enhanced NMR data in a more quantitative fashion, by plotting the relative integral, linewidth, and frequency shift values of these spectra as a function of time after injection. For the sake of convenience all these parameters are plotted normalized to the values they took 6 s after the sample's injection; a time chosen since it was observed that from this point onwards all the parameters followed an approximately exponential decay vs. time. Notice that the signal integrals do not follow a perfectly exponential behavior, especially immediately following the sample's injection. Here their values are smaller than expected; possible causes underlying this effect could relate to the fact that (i) the sample has not yet settled completely in the tube and air bubbles may still occupy a sizable fraction of the coil's volume; or (ii) radiation-damping phenomena could be counteracting the effects of the rf pulses used for the excitation [38] – especially given the very weak fields that were used in order to preserve the largest possible fraction of the enhanced magnetization along the z-axis. Still, these deviations are not severe, and a mono-exponential behavior of these integral values sets in after approximately 2.3 s, with a decay constant of 6.5 s (an independent inversion-recovery measurement from a sample with the same composition gave a T_1 constant of 7.5 s). The post-injection

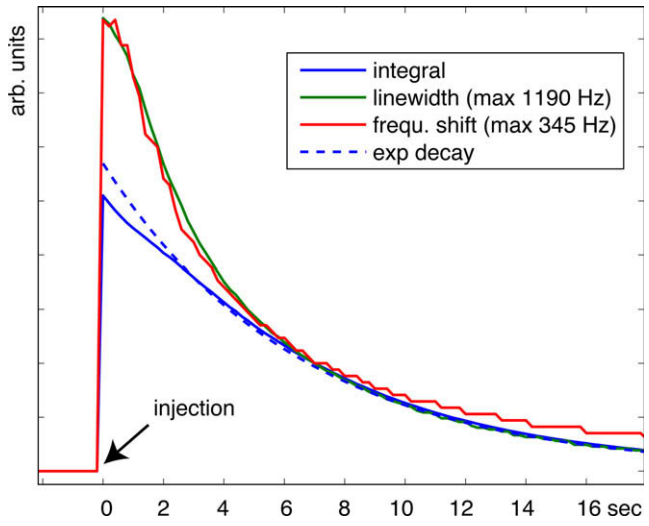

Fig. 2. Integral vs. time, linewidth vs. time, and frequency (of the maximum) vs. time dependencies of hyperpolarized water samples. All three plots are normalized at ~6 s after injection, in order to compare the decay behavior. A mono-exponential fit with T_1 = 6.5 s is shown as well (dashed line).

enhancement factor achieved by *ex situ* DNP was estimated from the mono-exponential decay of these signal integrals: a $K = 705$ enhancement then resulted *vis-à-vis* thermal polarization.

Interestingly, much more severe are the deviations from mono-exponentiality displayed by the remaining two observables measured in these DNP characterizations: the linewidth and the frequency shift of the hyperpolarized H_2O signals. While these parameters follow approximately the same exponential decay behavior as the signal's integral at times $\geqslant 6$ s after the sample's injection, they are considerably different at shorter intervals. The origins of these deviations are not entirely clear; it is known, however, that hyperpolarized sample line shapes may show a complex behavior immediately following their injection [39]. Part of this behavior could be due to inhomogeneities created upon flowing the sample into the NMR tube; for instance by the generation of a transiently concentrated sample, which gets diluted as the NMR tube is filled up and homogenized by the solvent being 'chased' over the first 1–1.5 s (with associated transient relaxation effects), and/or due to the presence of thermal gradients arising from the externally injected sample.

Fig. 3 shows a comparison of a noise spectrum at thermal polarization, with a series of ^{1}H noise spectra arising from the same DNP polarization-enhanced sample as a function of time. The thermally polarized ^{1}H noise spectrum was performed in order to identify the correct circuit tuning conditions [8,9], as well as to extract all the remaining parameters needed for the simulation of DNP-enhanced noise measurements. A simulation based on Eq. (4) with $K = 1$ (thermal polarization), $\vartheta = 1$ (room temperature probe), and $\lambda_r = 38.4\pi$ rad/s fitted the experiment best. With these results at hand, the progression of the spin-noise ^{1}H power spectra arising from DNP-enhanced water following the sample's injection into the NMR (Fig. 3) could be analyzed. Although the individual data strings leading to these spectra were digitized over 1 s, eight successive data sets had to be signal averaged for each measurement. In order to show the behavior of the noise spectra as a function of polarization decay, consecutive panels represent the spectra obtained from data strings starting at the indicated time after injection. As a result, the data are obtained from interleaved blocks. This overlap was unavoidable in order to show the decay of the noise signal with a reasonable SNR. Simulations of the resulting experimental data could then be performed on the basis of Eq. (4) with no fitting parameters: the enhancement factor $K = 705$ was extrapolated from Fig. 2; the radiation-damping constant was taken from the thermal noise measurement and divided by the dilution factor of 22 (concentration difference between the 100% H_2O sample and the DNP sample); and the T_1 value was derived from the exponential fit of the integrals as shown in Fig. 2. The exponential decay was considered to adjust both the linewidth and the frequency shift through the time course of the experiment, as indicated by Figs. 1 and 2. Each simulated spectrum is hence the result of an average of frequency-shifted and enhancement-adjusted noise spectra calculated according to Eq. (4), over the 8 s span involved in the experiment's signal averaging. Overall, a very good agreement results between these theoretical predictions and the experimental traces. The most evident feature in this time series is that, as the DNP-imparted spin polarization decays, the noise signal becomes narrower and smaller – eventually disappearing into the circuit noise. Indeed, at this dilution factor, the sample-generated noise effect is not observable on a thermally-equilibrated sample within such short signal-averaging times. Another notable agreement between the predictions and the experiments rests in the asymmetry displayed by the noise spectra within the first three experiments following the sample's injection. This asymmetry arises from the effects of the radiation-damping-derived frequency shift effects during the course of the experiment (noted in Fig. 1); as expected, these effects (and their consequences on the noise profiles) also diminish over time.

In observing these transient noise phenomena, it would have been particularly interesting to investigate situations where the protons are initially endowed with a negative polarization (thereby leading to a negative λ_r term in the denominator of Eq. (4)). The polarization could have been created by carrying out DNP on the opposite-polarizing transition; *i.e.*, by pumping microwaves onto the double-quantum instead of on the zero-quantum transitions [22]. Unfortunately, given the available hardware this option could not be realized (our source's 400 MHz bandwidth could not cover the necessary shift in microwave frequency). Still, we attempted to invert the enhanced polarization by applying a 180 degree pulse inside the NMR spectrometer, followed by a strong field gradient to dephase transverse magnetization which could have otherwise initiated a burst of signal due to radiation-damping feedback [13]. Even with such precaution, however, noise initiated a radiation-damping reaction, flipping the magnetization quickly back to its equilibrium position (observable as a burst in the detected signal). In fact, a recent report described multiple such spontaneous 'maser' bursts for dissolved hyperpolarized ^{129}Xe [40]; a very interesting effect which may be the signature of non-linear spin dynamics such as spectral clustering [41]. Only a single burst was seen in our ^{1}H DNP experiments; a fact which was attributed to the much shorter T_1 times compared to the noble-gas case [40]. Although much longer T_1 times could of course be explored in ^{13}C NMR, no such bursts were seen altogether in ancillary DNP-enhanced ^{13}C NMR experiments – not even a single one. This behavior, arising in spite of the very high polarization levels achievable in such systems (≈30–50 %), is likely a reflection of the very low radiation-damping constants involved in low-γ setups.

We highlight that the DNP approach leads to the enhanced detection of noise signals via the increase of the coupling with the coil. On a microscopic level, there may be difficulties in producing a fundamental physical picture that would delineate the difference between radiation-damping phenomena and genuine absorbed circuit noise and spin-noise effects, since the former are present in any measurement process [12]. DNP hyperpolarization can therefore also be used to examine the dynamic ranges of all these phenomena. The Nyquist treatment can be adjusted properly to include the effects of a large polarization and fits the experimental data very well with the major contribution arising from absorbed circuit noise under the conditions considered in this work.

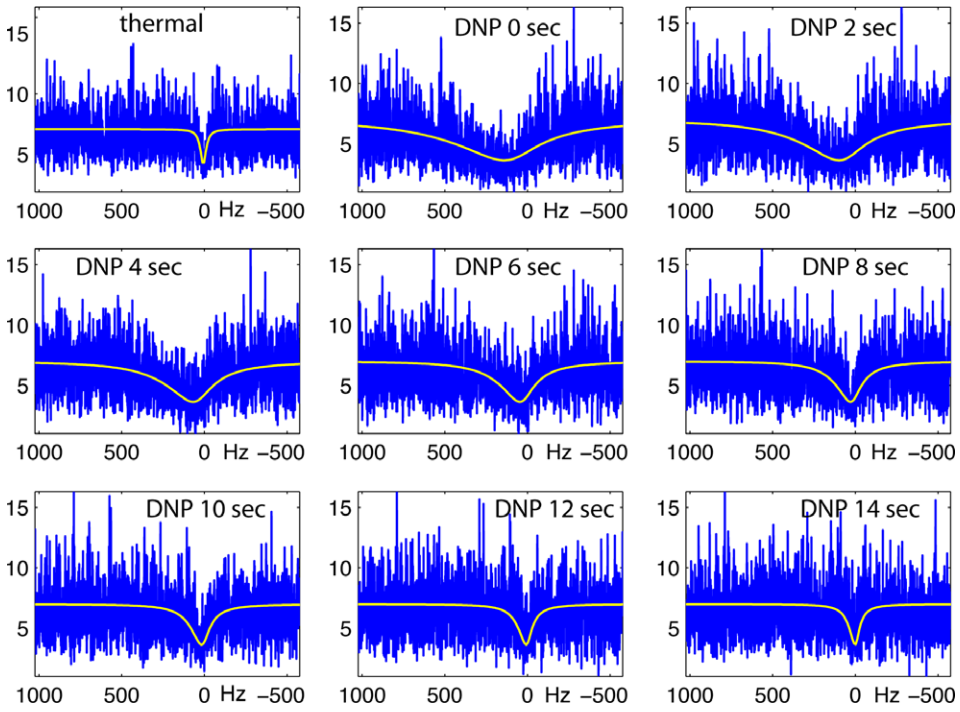

Fig. 3. Noise spectra (blue) and simulations (yellow) of a thermally polarized 100% water sample, and DNP polarization-enhanced samples (100 μL H_2O + 100 μL DMSO-d_6 + 2 mL D_2O) at the indicated times after injection. (For interpretation of the references to colour in this figure legend, the reader is referred to the web version of this article.)

5. Conclusion

The *ex situ* DNP approach usually employed to hyperpolarize dilute ^{13}C or ^{15}N spins in metabolites, can also give enhancement levels approaching 1000 for conventional ^{1}H NMR samples such as water. This effect in turn may open a number of interesting avenues to explore the physics of hyperpolarized high-γ spins in liquids. The present study reported a number of such features, with an emphasis on the detection of sample noise signals. It was demonstrated that these kinds of power spectra could be observed even from low-concentration samples, provided that these are pre-enhanced by DNP. This polarization enhancement leads to an increased coupling of the fluctuating signals with the reception circuit, thus enhancing the detected signals. The study of the noise processes in the presence of high polarization may allow one to better understand the interplay between genuine spin-noise phenomena, absorbed circuit noise, and the detection process, which is amplified by radiation damping. Using the Nyquist treatment, we have also shown that the contribution of spin-noise to the signals diminishes as polarization levels increase. Marked line broadening and frequency-shifting effects were also seen related to radiation-damping effects. Both the linewidth and the frequency shifts decayed together with the hyperpolarized sample's magnetization, although without exhibiting the polarization's nearly mono-exponential T_1-driven decay. Potential reasons underlying this behavior and related to sample inhomogeneities were put forward, and are the target of further research. Regardless of these deviations, there was excellent agreement between the overall features revealed by pulsed NMR regarding the post-DNP ^{1}H polarization behavior, and independent noise experiments. Multiple maser effects from spin-temperature inversion were also sought, but could not be found in these DNP-enhanced ^{1}H NMR experiments – most likely as a result of the short T_1 times involved.

We trust that liquid-state DNP experiments like the ones here reported can lead to a better understanding of many basic phenomena in NMR, such as the spin-noise and absorbed circuit noise mechanisms.

Acknowledgments

This research was supported by the Israel Science Foundation (ISF 447/09) and by the generosity of the Perlman Family Foundation. We are grateful to Drs. Mor Mishkovsky and Christian Bretschneider for help during this project. P.G. acknowledges the Weizmann Feinberg Graduate School and the French Ministry of Foreign and European Affairs (Lavoisier program) for a fellowship. NM acknowledges a research grant by FWF (The Austrian Science Funds) Project No. P19635-N17. A.J. acknowledges a research grant from the US National Science Foundation No. CHE 0554400, as well as a grant from the US–Israel Binational Science Foundation No. 2007157, and stimulating discussions with Tycho Sleator.

References

[1] F. Bloch, Phys. Rev. 70 (1946) 460.
[2] T. Sleator, E.L. Hahn, C. Hilbert, J. Clarke, Phys. Rev. Lett. 55 (1985) 1742.
[3] T. Sleator, E.L. Hahn, C. Hilbert, J. Clarke, Phys. Rev. B 36 (1987) 1969.
[4] M.A. McCoy, R.R. Ernst, Chem. Phys. Lett. 159 (1989) 587.
[5] M. Guéron, J.L. Leroy, J. Magn. Reson. 85 (1989) 209.
[6] S.A. Crooker, D.G. Rickel, A.V. Balatsky, D.L. Smith, Nature 431 (2004) 49.
[7] N. Müller, A. Jerschow, Proc. Nat. Acad. Sci. USA 103 (2006) 6790.
[8] D.J.-Y. Marion, H. Desvaux, J. Magn. Reson. 193 (2008) 153.
[9] M. Nausner, J. Schlagnitweit, V. Smrecki, X. Yang, A. Jerschow, N. Müller, J. Magn. Reson. 198 (2009) 73.
[10] H. Kovacs, D. Moskau, M. Spraul, Prog. Nucl. Magn. Reson. Spectrosc. 46 (2005) 131.
[11] L. Darrasse, J.-C. Ginfri, Biochimie 85 (2003) 915.
[12] D.I. Hoult, N.S. Ginsberg, J. Magn. Reson. 148 (2001) 182.
[13] A. Vlassenbroek, J. Jeener, P. Broekaert, J. Chem. Phys. 103 (1995) 5886.
[14] M.P. Augustine, Prog. Nucl. Magn. Reson. Spectrosc. 40 (2002) 111.
[15] H. Desvaux, D.J.Y. Marion, G. Huber, P. Berthault, Angew. Chem., Int. Ed. 48 (2009) 4341.
[16] M.S. Albert, G.D. Cates, B. Driehuys, W. Happer, B. Saam, C.S. Springer, A. Wishnia, Nature 370 (1994) 199.

[17] G. Navon, Y.-Q. Song, T. Room, S. Appelt, R.E. Taylor, A. Pines, Science 271 (1996) 1848.
[18] C.R. Bowers, D.P. Weitekamp, Phys. Rev. Lett. 57 (1986) 2645.
[19] T.C. Eisenschmid et al., J. Am. Chem. Soc. 109 (1987) 8089.
[20] T.R. Carver, C.P. Slichter, Phys. Rev. 92 (1953) 212.
[21] K.H. Hausser, D. Stehlik, Adv. Magn. Reson. 3 (1968) 79.
[22] A. Abragam, M. Goldman, Rep. Prog. Phys. 41 (1978) 395.
[23] W. Muller-Warmuth, K. Meise-Gresch, Adv. Magn. Reson. 11 (1983) 1.
[24] J.H. Ardenkjaer-Larsen et al., Proc. Natl. Acad. Sci. USA 100 (2003) 10158.
[25] J. Wolber et al., Nucl. Instrum. Methods Phys. Res. A 526 (2004) 173.
[26] V.S. Bajaj et al., J. Magn. Reson. 160 (2003) 85.
[27] K. Golman, R. In't Zandt, M. Thaning, Proc. Natl. Acad. Sci. USA 103 (2006) 11270.
[28] A.P. Chen et al., Magn. Reson. Med. 58 (2007) 1099.
[29] S.E. Day et al., Nat. Med. 13 (2008) 1382.
[30] F.A. Gallagher et al., Nature 453 (2008) 940.
[31] L. Frydman, T. Scherf, A. Lupulescu, Prod. Natl. Acad. Sci. USA 99 (2002) 15858.
[32] L. Frydman, A. Lupulescu, T. Scherf, J. Am. Chem. Soc. 125 (2003) 9204.
[33] L. Frydman, D. Blazina, Nat. Phys. 3 (2007) 415.
[34] M. Mishkovsky, L. Frydman, ChemPhysChem 9 (2008) 2340.
[35] M.H. Levitt, Concepts Magn. Reson. 8 (1996) 77.
[36] D.A. Torchia, J. Biomol. NMR 45 (2009) 241.
[37] S.Y. Huang, C. Anklin, J.D. Walls, Y.-Y. Lin, J. Am. Chem. Soc. 126 (2004) 15936.
[38] J.-H. Chen, A. Jerschow, G. Bodenhausen, Chem. Phys. Lett. 308 (1999) 397.
[39] H. Desvaux, D.J. Marion, G. Huber, L. Dubois, P. Berthault, Eur. Phys. J. Appl. Phys. 36 (2006) 25.
[40] D.J.Y. Marion, P. Berthault, H. Desvaux, Eur. Phys. J. D 51 (2009) 357.
[41] J. Jeener, Phys. Rev. Lett. 82 (1999) 1772.